J. Phys. B: At. Mol. Opt. Phys. **30** (1997) 309–318. Printed in the UK PII: S0953-4075(97)73442-4

Nonlinear coupling between rotation and internal vibration in simple molecular systems

Yibing Li and Estela Blaisten-Barojas

Institute for Computational Sciences and Informatics, George Mason University, Fairfax, VA 22030, USA

Received 10 April 1996, in final form 28 August 1996

Abstract. A Hamiltonian is proposed to describe the coupling between vibration and rotation in a molecular system. The time behaviour of such a system exhibits both regular and irregular motion for different energies and different values of the coupling parameter. There is a dramatic manifestation of the transition between the two types of dynamics that define parametric regions of regular and irregular behaviour. The Lyapunov exponent, phase portraits, Poincaré sections and power spectra are calculated. The computer simulations show that the vibrational anharmonicity favours the regular behaviour of the system.

1. Introduction

The study of complex irregular dynamics may be said to have started with the work of the French mathematician J H Poincaré at about the turn of the century. Although qualitative dynamics has been known to exist for a long time, its importance for a broad variety of molecular applications began to be appreciated only within the last decade. There are two main lines of research in this rapidly developing field: investigation of dissipative systems and research on Hamiltonian chaos. Concurrently, there has been enormous interest both within the mathematical community and among engineers and scientists to apply simple Hamiltonians to the description of a 'few' selected degrees of freedom relevant in complex systems. The field continues to develop rapidly, and its applications in material sciences are growing because of the fascinating changes in the time evolution of molecular systems [1–3].

Several Hamiltonian systems with two degrees of freedom are known to exhibit a transition from regular to chaotic motion as the energy of the system is increased. This is the case of the well studied two-dimensional Henon and Heiles system [4]. However, fewer studies have been undertaken which carefully examine the role played by the coupling parameters in a Hamiltonian system while the energy is kept constant. To be able to control these coupling parameters is one of the novel approaches of this technology.

In this paper we present a two-degrees-of-freedom Hamiltonian system which is suitable for the description of molecular vibration–rotation processes. In this model we assume that the two relevant variables of the motion are represented by a stretching vibration coupled with the rotation around an axis perpendicular to the vibrational displacement that passes through the oscillator equilibrium position. The coupling energy is $V_0(1 - \cos nq)$ [5] where the potential barrier V_0 is a function of the amplitude of vibration r and q is the angle of rotation. In this paper, we considered the case of $n = 4$, which is representative of a fourfold symmetry molecule or of a cubic trapping site. The time evolution of this model system is obtained by solving Hamilton's equations of motion numerically. Two parameters, the vibrational anharmonicity constant and the rotation–vibration constant, are changed along a surface of constant energy to observe the behaviour of a regular–chaos transition. We observe that the system is characterized by two chaotic regions separated by a regular region. The transition between the regions depends strongly on the value of the coupling parameters. It is important to understand how energy is shared and accommodated between the various active degrees of freedom and locked into the system. This is the thrust of the present study.

Hamiltonian models of this type are encountered in the literature for various values of n. A similar two-dimensional Hamiltonian system has been reported [6] although the authors did not consider the correlation between coupling constants and total energy. Other published work deals with the molecular vibration and rotation motions separately [7, 8]. Neglecting the interaction between the rotational and vibrational parts is justified with molecules in their ground rotational and vibrational states. When the molecules are externally excited (by light, for example) or when the system is at high temperatures, vibration and rotation are non-separable, as was shown recently [9].

2. Model Hamiltonian

A novel nonlinear Hamiltonian, suitable for the discussion of the coupling between the vibration and rotation of a two-degrees-of-freedom molecular system is chosen to be

$$H = \tfrac{1}{2}(\dot{r}^2 + r^2 + r^2\dot{q}^2) + kr^4 + gr^4(1 - \cos(4q)) \, . \tag{1}$$

The dynamical variables are: the vibration displacement from equilibrium r; the oscillator velocity $\dot{r}$; the rotation angle q and the angular velocity $\dot{q}$. Energy is given relative to the equilibrium energy of the system with zero angular momentum. The first three terms of (1) represent a harmonic oscillator with frequency $\omega = 1$ and mass $m = 1$ that rotates in a plane as a result of the vibration [10]. The fourth term indicates the anharmonicity in the vibration. The fifth term is responsible for the coupling between the vibration and the rotation degrees of freedom. This last term represents an anisotropic displacement of the system from equilibrium and accounts for changes in the angular momentum. Let us note that a cubic anharmonicity is absent in (1) to preserve the symmetry in the oscillation amplitude. In fact, the cubic anharmonic correction is zero for crystals with central symmetry. In quantum mechanical approaches to molecules, the anharmonic corrections to the harmonic energy usually include both cubic and quartic anharmonic terms. However, up to second order in perturbation theory, the total anharmonic correction to the energy depends quadratically on the cubic term and linearly on the quartic term.

A common model to account for hindrance of a planar rotation assumes [5] that the rotor has a potential energy

$$V = V_0(1 - \cos(nq)) \tag{2}$$

where V_0 is the height of the barrier and n is a degeneracy index identifying the number of symmetric equivalent saddles and valleys encountered by the rotor. The coupling term in our model Hamiltonian resembles this model. However, in our case the system rotates *only* when the amplitude of vibration is non-zero. Therefore, V_0 is not constant in time but rather becomes a function of the dynamical variable r. As stated in (1), in our model $V_0(r) = gr^4$ where g measures the strength of the coupling.

The following two cases are discussed in the next few paragraphs: $k = 1$ and $k = 0$. In the first case the vibration is anharmonic and in the second case the vibrator is harmonic.

The dynamical variables are $r,\ q,\ \dot{r},\ \dot{q}$. To solve Hamilton's equations of motion in these variables is inefficient. It is more convenient to search for a transformation of coordinates such that the oscillating terms in the Hamilton equations will not be present. We propose:

$$x = r\cos(q) \qquad y = r\sin(q)\,. \tag{3}$$

The Hamiltonian in (1) is thus transformed to (x, y) coordinates:

$$H = \tfrac{1}{2}(\dot{x}^2 + \dot{y}^2) + \tfrac{1}{2}(x^2 + y^2) + k(x^2 + y^2)^2 + 8gx^2y^2 \tag{4}$$

and the Hamilton equations are

$$\begin{aligned} x + 4k(x^3 + xy^2) + 16gxy^2 &= -\ddot{x} \\ y + 4k(y^3 + yx^2) + 16gyx^2 &= -\ddot{y}\,. \end{aligned} \tag{5}$$

Verlet's third-order finite difference method [11] was used to solve the above equations numerically with a time step of 10^{-3}. The numerical stability is validated by checking that the energy is kept constant.

3. Chaotic behaviour

The initial conditions of the dynamical variables needed to solve the equations of motion define different domains of total energy of the system. We have studied in detail cases for which the initial condition for angles $q = n\pi/2$ $(n = 0,\ 1,\ 2, \ldots)$ zeroes the coupling term of the Hamiltonian regardless of the value of g. Most of our simulations were performed with the initial condition $(x,\ y,\ \dot{x},\ \dot{y}) = (0,\ 1,\ 2,\ 3)$ which leads to an energy surface $E = 7$ for $k = 0$ and $E = 8$ for $k = 1$. This range of energies corresponds to an oscillator which can acquire amplitudes of vibration as large as $r = 4$.

Once the energy domain is fixed, for both cases $k = 0$ and $k = 1$, we solved the equations of motion for various values of the coupling parameter g. Once the trajectories were available it was possible to determine whether the behaviour was chaotic or not as a function of the parameter. To do this we investigated the behaviour of the Euclidean distance in phase space [12] between a parent trajectory and another trajectory obtained by slightly perturbing the parent trajectory at the initial time $t = 0$:

$$d(t) = \sqrt{(x_0 - x_1)^2 + (\dot{x_0} - \dot{x_1})^2\tau^2 + (y_0 - y_1)^2 + (\dot{y_0} - \dot{y_1})^2\tau^2} \tag{6}$$

where the set $(x_0,\ y_0,\ \dot{x_0},\ \dot{y_0})$ corresponds to the parent trajectory, $(x_1,\ y_1,\ \dot{x_1},\ \dot{y_1})$ represents the perturbed trajectory and τ is the time unit. The initial perturbation applied to the parent trajectory is denoted by d_0 and its value is set to $d_0 = 3 \times 10^{-5}$.

When the Euclidean distance between trajectories at short times behaves linearly with time, then the motion is said to be regular. However, for certain values of the coupling parameter g, the motion of our system departs from the linear behaviour and displays a growing exponential behaviour at short times. This dynamical instability is characteristic of chaotic motion and the short time behaviour can be characterized by the leading Lyapunov exponent λ defined by

$$\lim_{d_0 \to 0} d(t)/d_0 = \exp(\lambda t)\,. \tag{7}$$

Our system is very sensitive to the value of the coupling parameter and we varied it over a wide range of values for both cases $k = 0$ and 1. A typical $\ln(d(t)/d_0)$ versus time plot is given in figure 1 for $k = 0$ and $g = 0.2$. The value of the Lyapunov exponent is

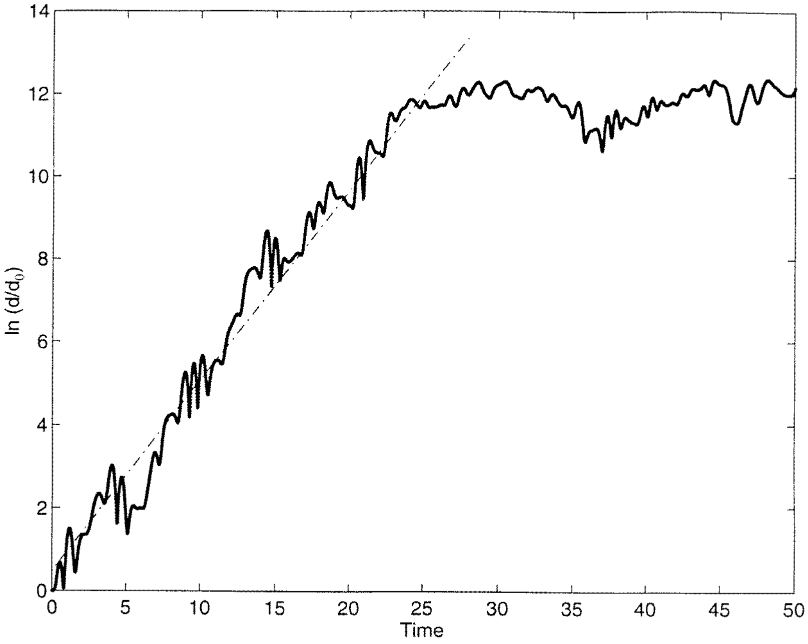

Figure 1. Time dependence of $\ln(d/d_0)$. The slope of the linear region is the Lyapunov exponent. The data correspond to $k = 0$, $g = 0.2$.

obtained from the slope of the best interpolated line (broken) at short times and is always positive. The dynamical correlation is lost at longer times, about $t = 20$ for the case shown in figure 1. We attribute the fluctuations in the short-time regime to the influence of non-leading exponents.

It is found that the Lyapunov exponent increases as g increases for $k = 1$. However, this behaviour is no longer valid for $k = 0$, as shown in table 1. The standard deviation in the values of λ are obtained from a sample of 10 different randomly perturbed trajectories all of which are obtained from the parent trajectory perturbed by the same d_0.

Table 1. The Lyapunov exponent versus g.

k	g	λ
0	0.75	0.97 ± 0.10
	0.5	0.53 ± 0.07
	0.4	1.31 ± 0.04
	0.2	0.48 ± 0.06
	0.1	0.57 ± 0.08
	0.05	0.51 ± 0.05
1	2.5	0.96 ± 0.04
	1.0	0.46 ± 0.05
	0.75	0.185 ± 0.03
	−0.375	0.33 ± 0.04
	−0.5	1.22 ± 0.03

4. Transition between regular and chaotic motion

Based on the previous analysis, and as a function of the parameter g, it is possible to define two thresholds between regular motion and chaotic motion. Below a threshold $g_{\min}$, $g < g_{\min}$, the system is chaotic with positive Lyapunov exponent. Above the threshold, $g > g_{\min}$, the system behaves regularly and the Euclidean distance between trajectories is a linear function of time. As g is increased further within the range $g_{\min} < g < g_{\max}$, the motion remains regular. However, if g is increased beyond $g_{\max}$, then the motion becomes chaotic again. This is depicted in figure 2. An almost continuous range of values of g was considered to produce this figure. The regular region $g_{\min} \leqslant g \leqslant g_{\max}$ shrinks as the total energy of the system increases. At even higher energies the system is chaotic at almost all values of g. On the other hand, at very low energies the system is chaotic only if $|g|$ is very large. In fact, for $E = 1.5$, the regular region spans between $-1.5 < g < 5$.

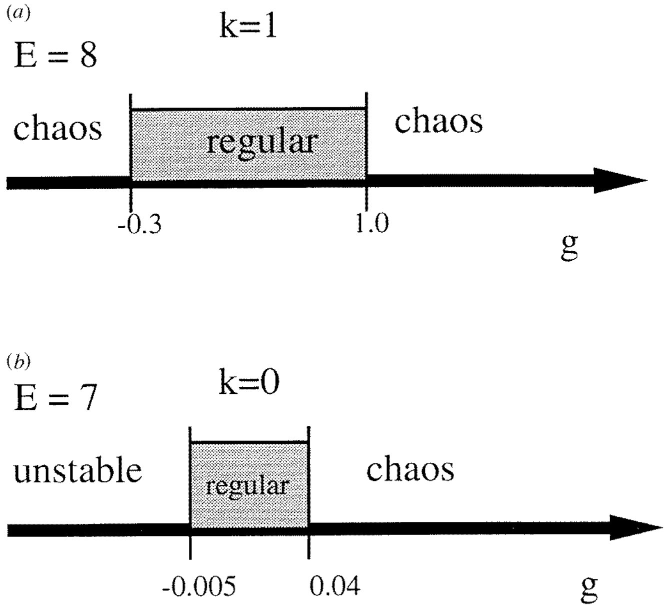

Figure 2. The transition region of chaos–order–chaos for (*a*) $k = 1$, $E = 8$ and (*b*) $k = 0$, $E = 7$. Parent trajectories were initiated with the same set of variables for (*a*) and (*b*).

Qualitatively, the motion of the system is quite similar to that of an intermittent rotor decoupled from an anharmonic vibrator when the strength of the coupling g is small (regular region) because the rotation is modulated by a shallow cosine function. The main effect of a small perturbation is to reverse the direction of rotation every time that $r = 0$. However, if the coupling strength is large, the system rotates or librates hopping between directions in a disconcerted fashion.

The harmonic vibration case obtained by setting $k = 0$ was also considered. We kept the same initial conditions as for the anharmonic case ($k = 1$) such that the total energy is now $E = 7$. We perform an analysis similar to that presented above illustrated in figure 2(*b*). The region of $g < -0.005$ is unstable because there are no minima of the potential energy. The region of regular motion $g_{\min} < g < g_{\max}$ is noticeably narrower than in the case

$k = 1$, indicating that the anharmonic term kr^4 *favours* the regularities of the system. The absence of vibrational anharmonicity shrinks the regular region of g. A similar observation was reported in the literature in which nonlinearities extend the range of existence of the periodic regime [13].

Let us now discuss the behaviour of other properties of the system as a function of g. For the case where $k = 1$, figures 3(*a*)–(*d*) illustrate our results for two values of the coupling: $g = -0.375$ and $g = -0.15$. The two left-hand figures (*a*), (*c*) depict the phase portrait (q, r) and the two right-hand figures (*b*), (*d*) correspond to Poincaré sections for $\dot{q} = 0$. As is evident from the phase portrait and Poincaré section, the system is chaotic for $g = -0.375$. As g is decreased the motion becomes regular, as shown in (*c*) and (*d*) for $g = -0.15$. In this second case the system is not chaotic and although its phase portrait is complex it exhibits regularities. Figure 3(*d*) shows that the points in the section are compressed to one line indicating that the system is nearly integrable [14].

Figures 4(*a*)–(*d*) show the power spectra of $r(t)$ and $q(t)$ for the case $k = 1$. Consistently, each power spectrum displays a set of well defined frequencies for $g = -0.15$ when the dynamics is regular. As chaos sets in ($g = -0.375$), the power spectrum converts to an irregular series of broadened lines emerging from an extended background.

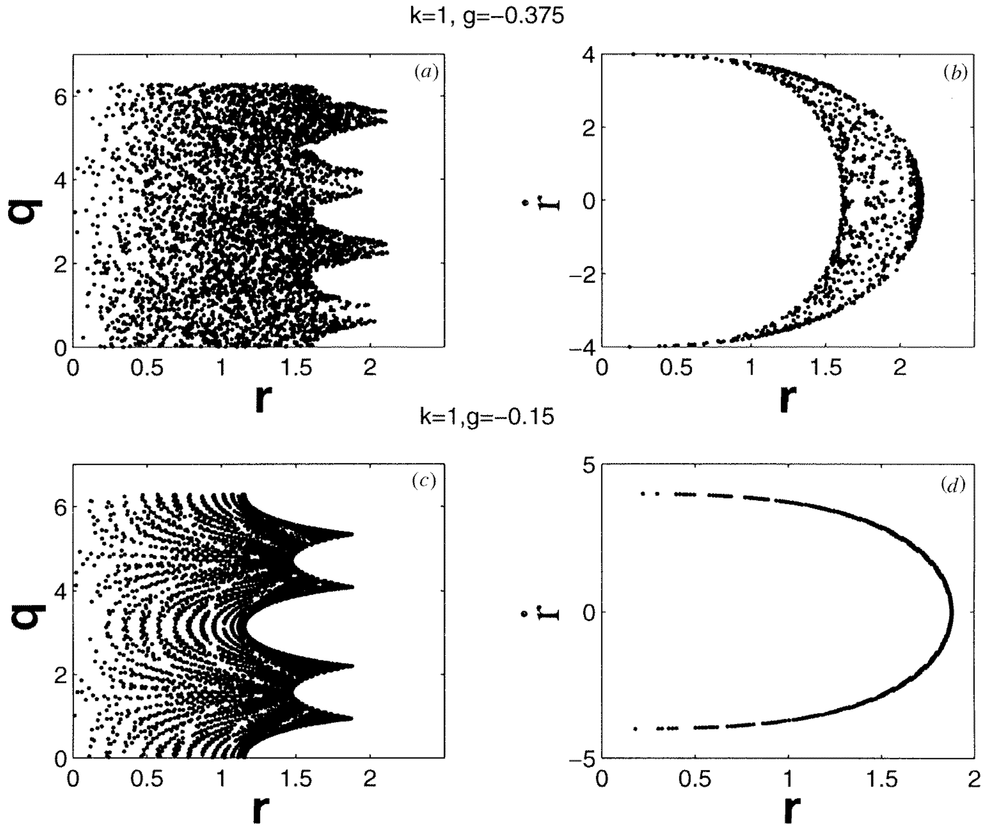

Figure 3. Phase portraits and Poincaré sections for $k = 1$ and different g values. (*a*) Phase portrait for $g = -0.375$; (*b*) Poincaré section for $g = -0.375$; (*c*) phase portrait for $g = -0.150$; (*d*) Poincaré section for $g = -0.150$.

The time evolution of the dynamical variables in our system is visualized qualitatively by a vibrating mass that undergoes a highly perturbed planar rotation around its equilibrium position. The rotation dies out when the mass passes through the equilibrium position. For the harmonic case, $k = 0$, figure 5 illustrates the time dependence of $r(t)$ for various values of the coupling g, whereas figure 6 shows the time series of $q(t)$. As is apparent in figures 5 and 6, the dynamical variables r, q display a periodic behaviour for small values of the coupling, i.e. $g \leqslant 0.0025$. However, for g values outside the regular region indicated in figure 2(*b*), i.e. $g = 0.025$, beats have formed in the $r(t)$ series and extra frequencies break the periodic pattern. When the coupling is even larger, $g = 0.055$, $r(t)$ and $q(t)$ present a complicated evolution. While vibrating the particle rotates and hops between the four angular minima, much as in a rotational diffusion motion although here energy is conserved. For strong coupling, $g = 0.125$ (top part of figure 6), it is apparent that for significant lengths of time the rotation is reduced to a vibration in one of the wells but then a hop brings the particle to a different angular position from where it continues a hindered rotation before being trapped into a new vibrating mode. In figure 7, we show the changes on the power spectrum of q as the value of g is decreased. A behaviour similar to the anharmonic case ($k = 1$, figures 4(*b*), (*d*)) is revealed. One distinct frequency is present only when the coupling g is in the regular region ($g = 0.0025$). As g increases many other frequencies erupt into the spectrum.

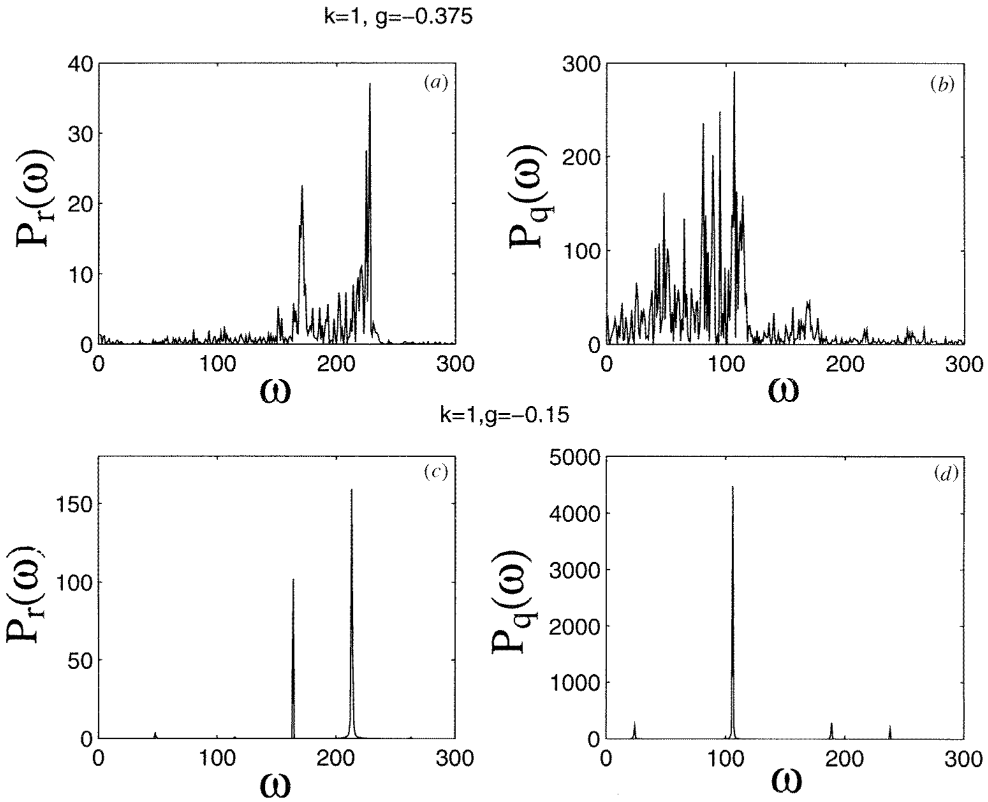

Figure 4. Power spectra of r and q for $k = 1$ and different g values. (*a*) $P_r(\omega)$ for $g = -0.375$; (*b*) $P_q(\omega)$ for $g = -0.375$; (*c*) $P_r(\omega)$ for $g = -0.150$; (*d*) $P_q(\omega)$ for $g = -0.150$.

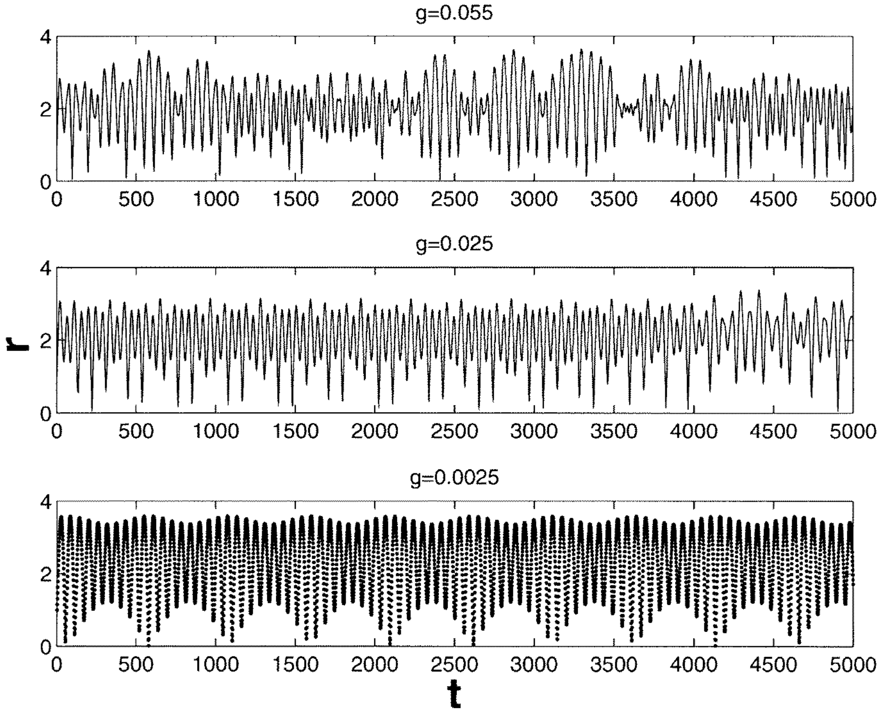

Figure 5. Time evolution of r for $k = 0$ and different values of g.

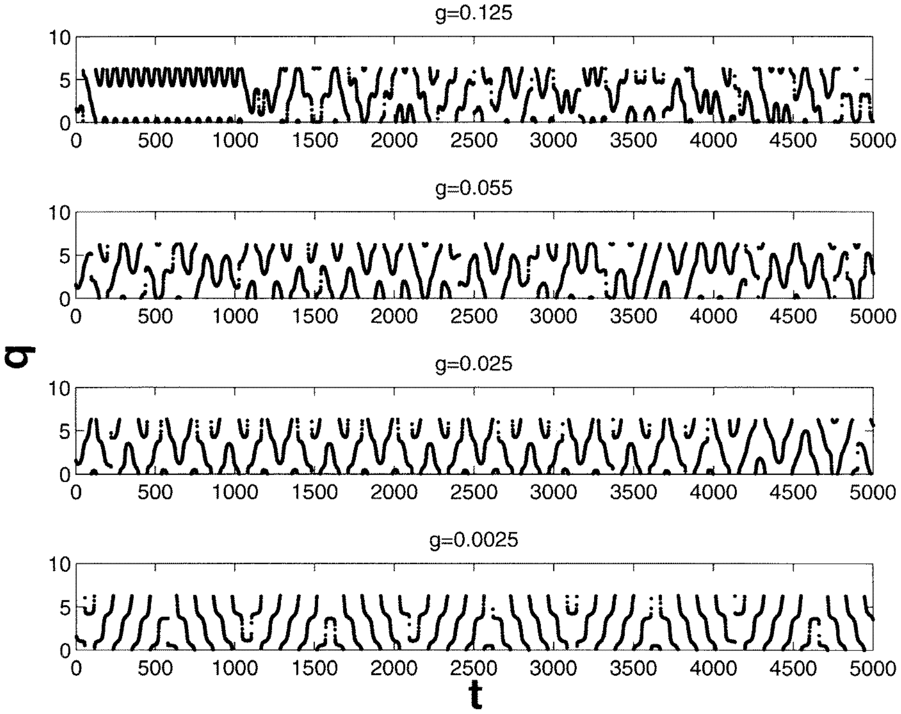

Figure 6. Time evolution of q for $k = 0$ and different values of g.

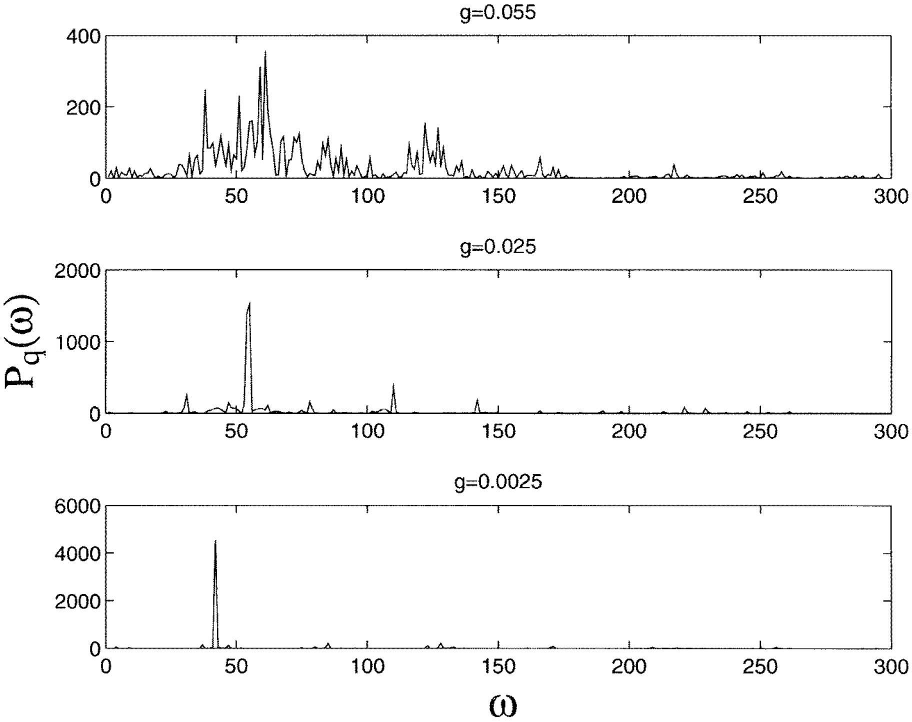

Figure 7. Power spectra of $q(t)$ for $k = 0$ and g decreasing from 0.055 to 0.0025.

5. Conclusion

The time evolution of the dynamical variables corresponding to a rotating–vibrating particle were analysed in detail. The Hamiltonian representing this system may be used to model two relevant degrees of freedom in molecular systems. We found that for fixed energy domains, changes of the coupling constant between vibration and rotation g generate two types of motion, regular if $g_{\text{min}} < g < g_{\text{max}}$ and irregular otherwise. Furthermore, the regular region in the parameter space (k, g) is wider if the anharmonic correction k is present, indicating that the anharmonic term favours the regularities in the dynamics of the system.

Acknowledgments

EBB acknowledges support from the Provost Office at George Mason University for funds allocated as a doctoral research assistantship to YL. Computations were performed on the cluster of workstations of the Institute for Computational Sciences and Informatics.

References

[1] Mills D L 1991 *Nonlinear Optics* (New York: Springer)
[2] Benedek B, Bilz B and Zeyher R 1983 *Statics and Dynamics of Nonlinear Systems* (New York: Springer)
[3] Gadzuk J W 1990 *Chemistry and Physics of Solid Surfaces VIII* ed R Vanselow and R Howe (New York: Springer) p 159

[4] Henon H and Heiles C 1964 *Astrophys. J.* **69** 73
[5] Pitzer K S 1951 *Faraday Soc. Disc.* **10** 66
Pitzer K S 1951 *J. Chem. Phys.* **5** 11
[6] Deng Z and Hioe F T 1985 *Phys. Rev. Lett.* **55** 1539
[7] Kunc J A 1990 *J. Phys. B: At. Mol. Opt. Phys.* **23** 2553
[8] Fernandez F M and Ogilvie J F 1992 *J. Phys. B: At. Mol. Opt. Phys.* **25** 1375
[9] Rothschild W G, Cavagnat R M and Maraval P 1993 *J. Chem. Phys.* **99** 8922
[10] Scheck F 1994 *Mechanics: From Newton's Laws to Deterministic Chaos* (New York: Springer)
[11] Verlet L 1967 *Phys. Rev.* **159** 98
[12] Kandrup H E and Mahon M E 1995 *Three-Dimensional Systems* ed H E Kandrup, S T Gottesman and J R Ipser (*Ann. NY Acad. Sci.* **751**) p 93
[13] Güemez J, Gutierrez J M, Iglesias A and Matias M A 1994 *Phys. Lett.* **190A** 429
[14] Reichl L E and Zheng W M 1987 *Directions in Chaos* ed Bai-lin Hao (Singapore: World Scientific) p 17